

**Allendeite and Hexamolybdenum: Two New Ultra-Refractory Minerals in Allende and Two Missing Links**

C. Ma\*, J.R. Beckett, and G.R. Rossman; Division of Geological and Planetary Sciences, California Institute of Technology, Pasadena CA 91125, \*chi@gps.caltech.edu.

**Introduction:** During our nano-mineralogy investigation of the Allende meteorite, we discovered two new minerals that occur as micro- to nano-crystals in refractory inclusions: Allendeite,  $\text{Sc}_4\text{Zr}_3\text{O}_{12}$ , a new Sc and Zr-rich oxide; and hexamolybdenum, (Mo,Ru,Fe), a Mo-dominant alloy. Allendeite, which may be an important ultra-refractory carrier linking Zr-, Sc- oxides and the more common Sc-, Zr-enriched clinopyroxenes (Cpx) in CAIs, hosts perovskite (Pv), spinel (Sp), Os-Ir-W-Mo alloys, and hexamolybdenum. The observation of two structurally and chemically distinct highly refractory, low-Pt alloy minerals not associated with Fe-Ni alloys provides the first direct physical evidence for at least two separate carriers of the highly refractory metals in CAIs. Hexamolybdenum links Os-rich and Pt-rich meteoritic alloys and may be a precursor of the latter. Both new minerals have been approved by the Commission on New Minerals, Nomenclature and Classification of the International Mineralogical Association (IMA 2007-027, 029).

**Occurrence, Chemistry and Crystallography:**

Allendeite and hexamolybdenum occur in a partially altered refractory inclusion  $\sim 70 \mu\text{m} \times 120 \mu\text{m}$  in section USNM 7554 (Fig. 1). Fig. 2 shows a single  $15 \times 25 \mu\text{m}$  crystal (revealed by electron backscatter diffraction (EBSD) orientation mapping) of allendeite with included Pv, Os-Ir-Mo-W alloy, and Sc-stabilized tazheranite (Taz; cubic zirconia). There are also linked or isolated 1-5  $\mu\text{m}$  irregular grains, coexisting with Pv, hexamolybdenum (Mo,Ru,Fe), and Os-, Ir-, Mo-, W-rich alloys. The inclusion is largely altered to nepheline (Ne), sodalite and Al-rich, low-Ti augite. Allendeite-Ne contacts are sharp but Pv within alteration, is often rimmed by ilmenite. We observed one grain of Mg-Al Sp in contact with allendeite, hexamolybdenum, and Pv, and rare Fe-Mg-Al Sp in altered regions.

Eight analyses of allendeite by EPMA yield (wt%)  $\text{ZrO}_2$  56.58,  $\text{Sc}_2\text{O}_3$  32.36,  $\text{TiO}_2$  5.47, CaO 2.74,  $\text{HfO}_2$  1.21, FeO 0.82,  $\text{Al}_2\text{O}_3$  0.70,  $\text{Y}_2\text{O}_3$  0.70,  $\text{V}_2\text{O}_5$  0.35 or  $(\text{Sc}_{3.01} \text{Ti}^{4+}_{0.44} \text{Ca}_{0.31} \text{Al}_{0.09} \text{Fe}^{2+}_{0.07} \text{Y}_{0.04} \text{V}^{3+}_{0.03})_{\Sigma 3.99} (\text{Zr}_{2.95} \text{Hf}_{0.04})_{\Sigma 2.99} \text{O}_{12}$ . No other elements with atomic number  $> 4$  were detected. Ti is proportional to Ca + Fe with a slope of 1.2, suggesting that  $\sim 20\%$  of the Ti may be trivalent. [1] observed a chemically similar phase in a grossite-bearing inclusion from the CH chondrite Acfer 182.

EBSD is used for *in-situ* non-destructive crystal structure determination at sub-micron scales. The

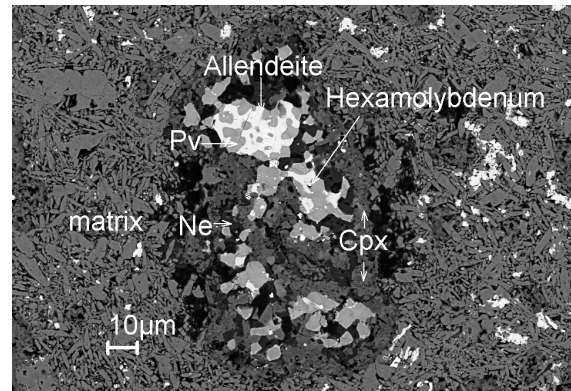


Fig. 1. Backscattered electron (BSE) image of the refractory inclusion containing allendeite and hexamolybdenum.

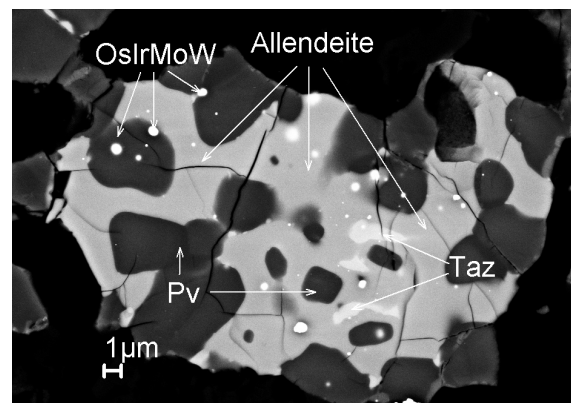


Fig. 2. Enlarged BSE image showing a single crystal of allendeite (cf. Fig. 1) with included Pv, tazheranite and Os-, Ir-, Mo-, W-rich alloys.

EBSD pattern of allendeite is an excellent match to the computed EBSD pattern and the cell parameters of synthetic trigonal,  $R\bar{3}$ ,  $\text{Sc}_4\text{Zr}_3\text{O}_{12}$  [2]. Zr and Sc are seven-coordinated to oxygen and randomly distributed on two sets of general sites [2]. Using cell parameters of [2] and our observed chemistry, we obtain a density of  $4.84 \text{ g/cm}^3$ . Allendeite is named for the locality Puelito de Allende, Chihuahua, Mexico, where the Allende meteorite fell in 1969.

We observed three hexamolybdenum inclusions in allendeite and a Zr-, Y-rich Pv (Fig. 3) and one  $1 \mu\text{m}$  inclusion in Pv and Cpx in Allende section USNM 3509HC12. The largest ( $1.2 \mu\text{m}$  diameter) grain consists of two parts. The upper, larger portion is a Mo-dominant phase and the lower brighter part is Ru-enriched. EPMA shows that the hexamolybdenum

portion of this crystal has an empirical formula  $\text{Mo}_{0.56}\text{Ru}_{0.24}\text{Fe}_{0.08}\text{Ir}_{0.07}\text{Os}_{0.03}\text{W}_{0.01}\text{Ni}_{0.01}$ , and the lower, brighter portion  $\text{Ru}_{0.41}\text{Mo}_{0.39}\text{Ir}_{0.10}\text{Fe}_{0.05}\text{Os}_{0.03}\text{W}_{0.01}\text{Ni}_{0.01}$ . The two smaller grains shown in Fig. 3 are too small for EPMA but the larger grain was confirmed to be hexamolybdenum by EBSD. SEM-EDS analysis yielded  $\text{Mo}_{0.44}\text{Ir}_{0.26}\text{Ru}_{0.19}\text{Fe}_{0.06}\text{W}_{0.04}\text{Os}_{0.01}$  (larger grain) and  $\text{Mo}_{0.82}\text{Ru}_{0.08}\text{Fe}_{0.04}\text{Os}_{0.03}\text{W}_{0.02}\text{Ir}_{0.01}$  (smaller grain).

The EBSD patterns can be indexed in terms of the  $P6_3/mmc$  structure exhibited by Ru and some intermediate Ru-Mo alloys. The best fit was achieved using cell parameters of synthetic  $\text{Mo}_{55}\text{Ru}_{45}$  [3]. Hexamolybdenum is hexagonal,  $P6_3/mmc$ ,  $a = 2.7506 \text{ \AA}$ ,  $c = 4.4318 \text{ \AA}$ ,  $V = 29.04 \text{ \AA}^3$  and  $Z = 2$ , with a calculated density of  $11.90 \text{ g/cm}^3$  via our observed chemistry. The name hexamolybdenum refers to the symmetry (primitive hexagonal) and composition (Mo-rich).

**Origin and Significance:** Zr-oxides are extremely refractory in nebular environments.  $\text{ZrO}_2$  is the highest temperature oxide to appear in condensation calculations for a cooling gas of solar composition [4]. Sc-, Zr-enriched Cpx are observed in CAIs and in some ultra-refractory inclusions [5-6] but previously reported meteoritic Zr oxides are minor grains or tiny inclusions [4,7] that may be exsolution phases rather than primary condensates or evaporative residues. Allendeite, a Zr-rich oxide, and Taz are well posed as sensors of conditions associated with their formation and, by extension, those of other ultra-refractory phases. Allendeite, Pv, and Taz all contain significant amounts of Zr, Sc, Al, Ca, Y,  $\text{Ti}^{4+}$  and possibly  $\text{Ti}^{3+}$ , so it is possible to construct exchange reactions with co-existing phases to constrain temperature, oxygen fugacity and/or the partial pressures of vapor species.

Allendeite is probably destroyed through reactions with other phases. For example, the relatively common Zr-, Sc-enriched Cpx in type A CAIs and in the mantles of type B1s [5,8] could reflect a precursor Zr-Sc oxide that dissolved into the melt with some of the Zr and Sc being subsequently incorporated into crystallizing Cpx. The Sc/Zr ratio of such a Cpx depends on Sc/Zr in the dissolving phase assemblage, how much diffusion occurred in the liquid prior to crystallization of the Cpx ( $\text{Sc}^{3+}$  likely diffuses faster than  $\text{Zr}^{4+}$ ), and the ratio of the Cpx/liquid partition coefficients for Sc and Zr. Taking the effective Cpx-liquid partition coefficients for Zr (1.1) and Sc (2.8) derived by [8] for core Cpx in type B1 inclusions as approximately correct for Sc-, Zr-rich Cpx, leads to  $\text{Sc}_2\text{O}_3/\text{ZrO}_2$  in initially crystallizing Cpx of  $\sim 1.5$  if no significant diffusion of Sc relative to Zr occurred in the liquid, in reasonable agreement with  $\text{Sc}_2\text{O}_3/\text{ZrO}_2$  (0.8-4.7) in Cpx associated with Zr-, Sc-rich Pv in compact type As [5].

Since allendeite and Pv have low  $\text{Y}_2\text{O}_3/\text{Sc}_2\text{O}_3$ , we would also expect low  $\text{Y}_2\text{O}_3/\text{Sc}_2\text{O}_3$  in the crystallizing Cpx, also as observed.

A wide variety of refractory metal alloys are observed in Fremdlinge or opaque assemblages of CAIs [9] but these probably formed through oxidation/sulfidation at low temperatures of Fe-Ni-rich alloys, possibly leading to exsolution of the observed refractory alloys [9]. Refractory metal nuggets are also observed included in CAIs but these are usually Os-Ir-rich or enriched in Pt, a relatively volatile noble metal, and/or Fe-Ni [10-11], indicative of more evolved alloys. Pt, Fe, and Ni contents of the hexamolybdenum and Os-Ir-W alloys in the Fig. 1 inclusion

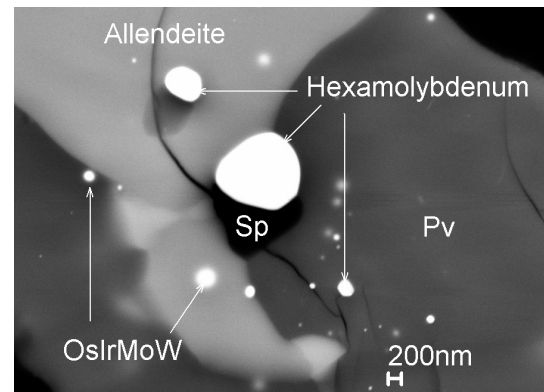


Fig. 3. BSE image showing a portion of Fig. 1 containing hexamolybdenum with allendeite, perovskite, and Os-Ir-Mo-W alloys.

are quite low, leading to the possibility that the alloys are relatively pristine examples of nebular refractory alloys that can yield insight into early nebular processes. [12] inferred that early condensation of refractory elements involved at least three different carriers. We suggest that two of these involved Os-rich alloys and Mo-, Ru-rich hexamolybdenum and its descendants. From a condensation perspective, continued exposure of hexamolybdenum to a cooling gas would likely lead to a reaction to form Pt-rich alloys with the destruction of hexamolybdenum.

**References:** [1] Weber D. and Bischoff A. (1994) *GCA* 58, 3855. [2] Rossell H.J. (1976) *J. Solid State Chem.* 19, 103. [3] Anderson E. and Hume-Rothery W. (1960) *J. Less-Common Metals* 2, 443. [4] Grossman L. (1973) *GCA* 37, 1119. [5] El Goresy A. et al. (2002) *GCA* 66, 1459. [6] Simon S.B. et al. *GCA* 63, 1233 (1999). [7] Hinton R.W. et al. (1988) *GCA* 52, 2573. [8] Simon S.B. et al. (1991) *GCA* 55, 2635. [9] Blum J.D. et al. (1989) *GCA* 53, 543. [10] Lin Y. et al. (1999) *Chinese Sci. Bull.* 44, 725. [11] Wark D.A. (1986) *EPSL* 77, 139. [12] Sylvester P.J. et al. (1993) *GCA* 57, 3763.